IEEE Access
Multidisciplinary ⋮ Rapid Review ⋮ Open Access Journal

Date of publication xxxx 00, 0000, date of current version xxxx 00, 0000.

Digital Object Identifier 10.1109/ACCESS.2017.Doi Number

Rapid Design of 3D Reflectarray Antennas by Inverse Surrogate Modeling and Regularization

Slawomir Koziel[1,2], Fellow, IEEE, Mehmet Ali Belen[3], Alper Caliskan[4], and Peyman Mahouti[5]

[1]Engineering Optimization & Modeling Center, Department of Technology, Reykjavik University, Menntavegur 1, 101 Reykjavik, Iceland
[2]Faculty of Electronics, Telecommunications and Informatics, Gdansk University of Technology, Narutowicza 11/12, 80-233 Gdansk Poland
[3]Department of Electrical and Electronic Engineering, İskenderun Technical University, 31200 Hatay, Turkey
[4]Department of Electronic and Communication Engineering, Yildiz Technical University, 34000 İstanbul, Turkey
[5]Department of Aviation Electronic, Yildiz Technical University, 34000, Istanbul, Turkey

Corresponding author: Slawomir Koziel (e-mail: koziel@ru.is).

The authors would like to thank Dassault Systemes, France, for making CST Microwave Studio available and Signal Processing for Computational Intelligence Group in Informatics Institute of Istanbul Technical University for providing computational resources. This work is partially supported by the Icelandic Centre for Research (RANNIS) Grant 206606, and by National Science Centre of Poland Grant 2020/37/B/ST7/01448.

ABSTRACT Reflectarrays (RAs) exhibit important advantages over conventional antenna arrays, especially in terms of realizing pencil-beam patterns without the employment of the feeding networks. Unfortunately, microstrip RA implementations feature narrow bandwidths, and are severely affected by losses. A considerably improved performance can be achieved for RAs involving grounded dielectric layers, which are also easy to manufacture using 3D printing technology. Regardless of the implementation details, a practical bottleneck of RA design is the necessity of independent adjustment of a large number of unit cells, which has to be carried out using full-wave electromagnetic (EM) simulation models to ensure reliability. The associated computational costs are extraordinary. A practical workaround is the incorporation of surrogate modeling methods; however, a construction of accurate metamodel requires a large number of training data samples. This letter introduces an alternative RA design approach, where the unit cells are adjusted using an inverse surrogate model established with a small number of anchor points, pre-optimized for the reference reflection phases. To ensure solution uniqueness, the anchor point optimization involves regularization, here, based on the minimum-volume condition for the unit cell. The presented approach reduces the computational cost of RA design to a few dozens of EM analyses of the cell. Several demonstration examples are provided, along with an experimental validation of the selected RA realization.

INDEX TERMS Antenna design; reflectarrays; surrogate modeling; inverse modeling; EM-driven design; regularization.

I. INTRODUCTION

Reflectarrays (RAs) have recently become recognized as attractive approaches to high-performance antenna implementation [1]-[3]. Their distinctive advantage is a possibility to realize pencil-beam patterns without the necessity to involve expensive feeding networks [4], which is achieved by assigning appropriate reflection phases to their constitutive elements (referred to as unit cells). Some of RA application areas include satellite communications, vehicular radars, and earth stations [5]-[7]. Reflectarrays can be developed using stacked rectangular metallic components [8], ring patches [9], or parallel dipoles [10]. More involved implementations enabling beam steering [11], inflatable RAs [12], or amplifying RAs [13], have been reported as well.

The most popular RA realizations involve microstrip technology (MRAs), which are cheap and easy to manufacture. At the same time, MRAs are inherently narrowband, affected by the losses (both conductor and surface-wave-related), and exhibit significant mutual coupling between the unit cells. Most of these issues can be mitigated with the unit cells implemented as grounded dielectric layers [14]. The required reflection phase can be obtained by varying the cell thickness. At the same time, dielectric-layer-based RAs are straightforward to manufacture using the 3D printing technology.

Despite their advantages, practical design of RAs is a time-consuming process due to the necessity of adjusting geometry and material parameters of a large number (typically a few hundreds) of unit cells to ensure their appropriate reflection phases. For the sake of reliability, this

has to be carried out using full-wave electromagnetic (FW-EM) models, [15], [16] such as Method of Moment (MOM) [16], Finite-Difference-Time-Domain (FDTD) [17] and Finite-Element-Method (FEM) [18], used to perform accurate evaluation of the design. However, due to large amounts of memory needed and significant computation time, high computational expenses would be accrued in these approaches. Thus, these methods might not be practical to be used for large scale antenna design or optimization, most especially for designs such as RAs.

Although there are challenging problems in design of RAs that include handling conflicting goals such as size and operating band, the most challenging part of RA design is the adjustment of geometrical parameters of the unit elements. RAs are realized using designs of complex geometrical shapes (unit elements) which can satisfy the requested performance criteria owing to their design nature with large number of degrees of freedom (DoFs). With the mentioned DoFs, RA unit elements can potentially provide a highly effective control over the reflection phase of the incoming EM waves to the unit elements [19-25]. Unfortunately, handling of RAs that incorporate such complex unit cells is usually extremely difficult and they force the designer to use rigorous numerical optimization, which are extremely computationally expensive tasks. In most cases, even if the designer uses a medium-level mesh density in the computational model, at the cost of losing accuracy, it is actually infeasible when conducted directly at the level of FW-EM model of the entire array where this process might take up to months or years to complete [19]. In order to have the optimal design variables of each unit element, designer must precisely know the behaviour and characteristics of both the unit cell (w.r.t parameters such as geometry/size material type etc.) and the illumination (e.g., the polarization, operation band, angle of arrival of the incident EM wave etc) [22], [23]. These can be analytically calculated only for RA designs with simple unit cells featuring a few DoFs [26], [27]. An alternative way is to use scattering matrices with respect to performance response's lookup tables (LUTs) using FW-EM simulation tools [28], [29]. However, it should be emphasized that the generation of such LUTs is not a computationally efficient or feasible task in RAs with complex unit cell designs due to the large number of unit cell DoFs [19], [30].

To expedite the process, surrogate modelling methods are often employed [31]-[36]. Unfortunately, a construction of a sufficiently accurate and design-ready model normally requires a large number of training data samples, typically 2,000 and beyond [34], [35]. The costs associated with the acquisition of the respective EM data is therefore significant. A recently published approach involving a forward modelling approach based on multi-layer perceptron with automated adjustment of the network architecture allows to reduce the number of samples to 500 [37]. However, the method of [37] is a forward based approach, which requires optimization of the surrogate to adjust dimensions of each element. Also it is worth mentioning that the cell optimization is a constrained task, which has to handle several objectives. Herein, a novel inverse modelling approach is proposed, which is entirely different than the methodology described in [37]. The method is not only dramatically more efficient (by about an order of magnitude) than the forward surrogate modelling approaches, but also allows for a direct rendition of optimized cells that exhibit required reflection phases and correspond to minimum weight of the array. Consequently, the methodology introduced in this paper simplifies the RA design process while being computationally more efficient. In order to present the superiority of the proposed approach to the recent forward-modeling-based technique of [37], the same RA unit element example is used in both works. It should be explained that this work used two different meanings for the term 'cost': (1) the computational cost (time) of overall design optimization process of a large or medium-size RA design. Here, for the sake of comparison, the results of two approaches are studied: (a) a traditional direct full-wave simulation-based method, (b) the proposed inverse surrogate-model-based technique; (2) the second meaning of the 'cost' is the cost function that quantifies the requested reflection phase and the volume of the RA unit element as defined in Eq. 1. The function is defined to achieve a RA design featuring the lowest possible volume and weight alongside of the highest possible focusing performance. Our methodology is based on inverse surrogate modelling, with the metamodel established using a small number of anchor points, obtained by optimizing the unit cell for specific target reflection phases within the range of interest. The uniqueness of solution is ensured through the incorporation of the regularization term, which enforces minimum physical size (volume) of the cell. The presented technique has been illustrated using several unit cells of different complexities. The average cost of RA design corresponds to only a few dozens of EM analyses of the unit cell, which is at least an order of magnitude lower than the typical cost of surrogate-assisted methods reported in the literature. Experimental validation of the selected RA realization has been discussed as well to supplement the numerical results.

II. REFLECTARRAYS: THE CONCEPT AND EM-DRIVEN DESIGN

Figure 1 shows a conceptual illustration of a reflectarray (RA) alongside of the proposed approach flow chart diagram. The radiation pattern of the array can be controlled by adjusting the reflection phases of the unit cells, which are antenna elements with either open- or short-circuit termination [37]. The said phases are to compensate for the path length differences between the feed and individual elements, and to realize the pattern of a required properties (e.g., narrow beam with low sidelobe levels). Some of the attractive properties of the RA include light weight, low cost, low volume, easy manufacturing, and no need for a feeding network. Also, RAs enable realization of high gain and high efficiency (the latter due to the lack of feed-related losses).

Practical design of RAs is a challenging endeavor due to the necessity of adjusting the properties of a large number of unit cells, typically, several hundreds. Regardless of the implementation technology (microstrip [8], grounded dielectric

[32]), each unit cell is described by several adjustable parameters, optimization of which is critical to obtain the required properties, here, the reflection phase. For simple cell architectures, it is possible to use analytical methods [38]-[40]. An alternative are lookup tables (LUTs) generated through extensive EM simulations [41]. Perhaps the most practical approach are surrogate-assisted methods [42], where a fast replacement model of the unit cell is constructed using sampled EM simulation data, and re-used to adjust the unit cell parameters for the entire RA. The mentioned methods are associated with significant computational expenses, typically measured in thousands of EM analyses of the unit cell [34], [35].

III. RAPID RA DESIGN USING INVERSE SURROGATES

This letter proposes a novel approach to RA design involving inverse surrogate modeling of the unit cell. Below, we explain and elaborate on the concept and implementation of the presented method. Illustration examples are provided in Section IV, whereas Section V discusses experimental validation of the specific RA design obtained using our technique.

A. UNIT CELL GEOMETRY AND DESIGN GOALS

To illustrate the concepts discussed in this section, a dielectric-layer-based unit cell element, which was used as a design example for a forward surrogate modeling approach in [37] is taken as a case study. We will denote by $\boldsymbol{x} = [x_1 \ldots x_n]^T$ the adjustable parameters of the cell, and by f the frequency. The EM-simulated reflection phase of the cell fill be denoted as a function $P_{\rm EM}(\boldsymbol{x},f)$. The physical size of the cell, specifically, its volume, will be denoted as $V(\boldsymbol{x})$. For the example in Fig. 2, we have $\boldsymbol{x} = [\varepsilon_r\ h\ a]^T$, and $V(\boldsymbol{x}) = [b^2 + ab + a^2]h/3$, where b (the cell base size) is normally fixed.

Design of RA requires identifying a parameter vector that ensures a target reflection phase $P(\boldsymbol{x},f_0) = P_t(f_0)$, for $P_{t.\min} \le P_t \le P_{t.\max}$, so that, normally, $P_{t.\max} - P_{t.\min} = 360$ degrees, where f_0 is the RA operating frequency. The latter is to ensure a sufficient flexibility of the cell in terms of realizing the required range of phases. The process has to be repeated for a large number of P_t values, depending on the RA size.

The most popular design approaches involve surrogate models of the unit cells, established over a domain X, defined by the lower and upper parameter bounds $\boldsymbol{l} = [l_1 \ldots l_n]^T$, and $\boldsymbol{u} = [u_1 \ldots u_n]^T$, respectively, determined by technology limitations (e.g., realizable range of permittivity, etc.). The bounds are broad in order to ensure the attainability of the target reflection phases within the range from $P_{t.\min}$ to $P_{t.\max}$. Needless to say, constructing the cell models over large spaces is expensive. As mentioned earlier, it requires many hundreds or even thousands of EM analyses of the cell to create a sufficiently extensive training data set.

B. DESIGN OPTIMALITY. REGULARIZATION

This work offers an alternative approach to cell modeling, which is elaborated on in Section III.*C*. Its foundation is the concept of cell optimality, supported by regularization. We consider the following task

$$\boldsymbol{x}^* = \arg\min_{\boldsymbol{x}\in X} \left\{ V(\boldsymbol{x}) + \beta[P_t(f_0) - P(\boldsymbol{x}, f_0)]^2 \right\} \qquad (1)$$

in which the primary objective is to ensure the minimum size of the cell while enforcing the required reflection phase. Note that the phase condition $P(\boldsymbol{x},f_0) = P_t(f_0)$ is a secondary goal, controlled implicitly using the penalty function approach [43]. The penalty coefficient should be sufficiently large to ensure the said enforcement (here, we use $\beta = 10^3$). The advantage of formulation (1) is that it guarantees the uniqueness of solution as long as the overall number on conditions imposed on the cell parameters (both phase- and volume-related) is larger than the parameter space dimensionality, which is normally the case. At the same time, minimum-volume design is preferable to ensure low weight and low fabrication cost of the RA. Note that (1) implicitly realizes a regularization scheme, which is essentially the incorporation of additional conditions (here, size-related) to ensure design uniqueness.

The above formulation of the problem is in contrast to conventional methods, where the objective is to yield the target phase. With such an approach, uniqueness of the design is not guaranteed. Consequently, the surrogate model has to be constructed over the entire parameter space, which incurs excessive CPU costs. Some sort of uniqueness is often implied at the RA design stage by aggregating the phase- and size-related objectives [37], yet it is only a partial solution.

C. ANCHOR DESIGNS AND INVERSE SURROGATE MODEL

Our goal is to construct an inverse surrogate model that directly yields unit cell parameter vectors corresponding to the required reflection phase values, without the necessity of further tuning of the cell.

Consider a sequence of target phases $P_{t.k}$, $k = 1, \ldots, N$, uniformly distributed within the range $[P_{t.\min}\ P_{t.\max}]$, i.e., we have, $P_{t.k} = P_{t.\min} + k[P_{t.\max} - P_{t.\min}]/(N-1)$. Let $\boldsymbol{x}^{(k)} = [x_1^{(k)} \ldots x_n^{(k)}]^T$ be the optimum cell designs found by solving the problem (1) for $P_t(f_0) = P_{t.k}(f_0)$, $k = 1, \ldots, N$, referred to as the anchor vectors. The task (1) is solved directly at the EM simulation level using the trust-region (TR) gradient-based algorithm with numerical derivatives [44], and rank-one Broyden formula [45] employed to update the sensitivity matrix from the second iteration of the algorithm on. With this method, the optimization cost is low, typically less than ten EM analyses of the unit cell.

Let $I(P,\boldsymbol{P}_t,\boldsymbol{y}) : X \to X$ be the function that interpolates the data set $\boldsymbol{P}_t = [P_{t.1} \ldots P_{t.N}]$, $\boldsymbol{y} = [y_1 \ldots y_N]$ for any value of P within the range $P_{t.\min}$ to $P_{t.\max}$ (note that $P_{t.1} = P_{t.\min}$, and $P_{t.N} = P_{t.\max}$). Here, we use cubic splines [46]. The inverse surrogate S_I is defined as

$$S_I(P) = \left[I(P, \boldsymbol{P}_t, \boldsymbol{y}_1) \ldots I(P, \boldsymbol{P}_t, \boldsymbol{y}_n) \right]^T \qquad (2)$$

where

$$\boldsymbol{y}_k = \left[x_k^{(1)} \ldots x_k^{(N)} \right]^T \qquad (3)$$

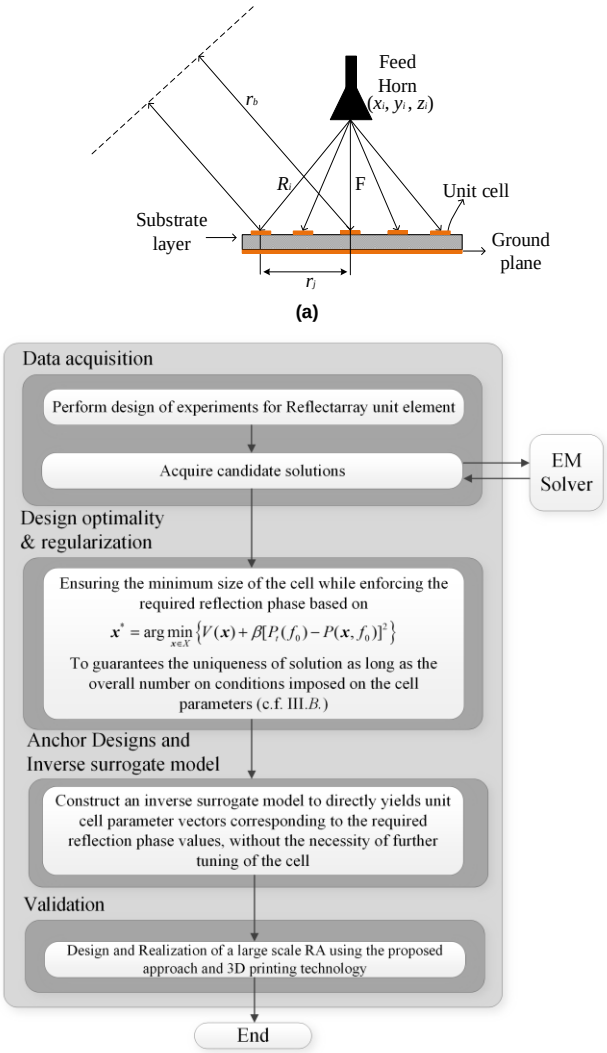

FIGURE 1. (a) Conceptual illustration of a Reflectarray, (b) flow chart diagram of the proposed approach.

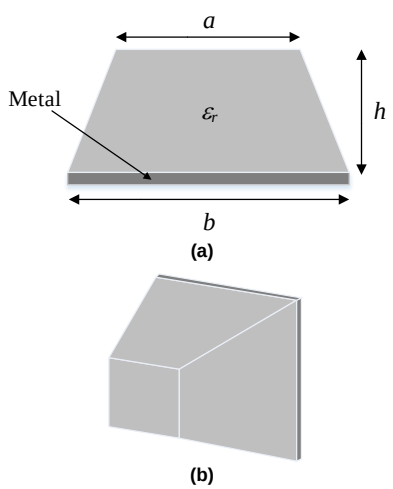

FIGURE 2. Example RA unit cell: (a) parameterized side view, (b) perspective view.

Recall that $x_k^{(j)}$ is the k^{th} component of the anchor vector $\boldsymbol{x}^{(j)}$. The inverse model S_I directly returns the optimum (here, minimum-volume) unit cell design that produces the required reflection phase P. In practice, the number of anchor designs necessary to ensure sufficient accuracy of the model (e.g., better than 1°) is a few, typically five to eight. Thus, the overall computational cost of constructing the surrogate (and, the RA design) is only a few dozens of EM simulations of the unit cell.

IV. ILLUSTRATION EXAMPLES

This section discusses three examples of unit cells, their inverse modeling, and applications to design of reflectarrays. In this work, dielectric resonator type antenna has been considered, which has shown a great potential [47]-[53]. The reasons for selecting a dielectric resonator-based unit element as follows

(i) The unit elements in this work are based on [14] where a grounded dielectric layer with variable thickness is used as a reflecting surface in order to mitigate the disadvantages of microstrip reflectarray designs such as narrow-band radiation and significant mutual couplings between microstrip elements printed on standard substrates. Furthermore, the conductor and surface wave loss are severe for microstrip implementations.

(ii) The ease of manufacturing of these elements due to their compatibility with 3D printers.

(iii) Owing to the unique capabilities of 3D printers, it is possible to manufacture unit elements in a way to precisely control their volume and height, in particular, to comply with specific dimensions developed to obtain the minimum array weigh.

Here, it should be emphasized that the studied unit elements would present lower computational requirements than most of more involved elements reported in the literature. However even with this level of simplicity, the total computational budget required for large-scale design optimization of a RA directly using FW-EM tools is dramatically higher than the proposed inverse surrogate based approach. Here, it should also be emphasized that even in the case of a simple design element such as the one considered in the work, the proposed approach can make a significant difference in terms of the total computational efficiency of design optimization process, as indicated in Table 1. Needless to say, the computational benefits would be even more pronounced for more involved unit elements.

A. EXAMPLE 1: SINGLE-LAYER UNIT CELL

We consider the unit cell shown in Fig. 2. In this case, the frequency of interest is f_0 = 10 GHz. The parameter b = 15 mm is fixed, and the design space for the parameters $\boldsymbol{x} = [\varepsilon_r\ h\ a]^T$, is $\boldsymbol{l}$ = [1.3 2.0 2.0]^T, and $\boldsymbol{u}$ = [2.7 20.0 15.0]^T. Here, seven anchor designs were found by solving (1), corresponding to $P_{t,k}$ = –90°, –150°, …, –450°, at the total cost of fifty EM simulations of the cell. As it turns out, the minimum-volume designs are obtained for ε_r = 2.7, and a = 2.0 mm in all cases.

The optimum values of parameter h are $\boldsymbol{y}_2$ = [3.09 5.20 7.08 8.86 10.69 12.64 14.68] mm. Consequently, the inverse model takes the form of $S_I(P)$ = [2.7 $I(P,\boldsymbol{P}_t,\boldsymbol{y}_2)$ 2.0]^T (cf. Fig. 3). The average value of the absolute error of the model, estimated using the independent set of 50 random test samples, is 0.1°, which is more than sufficient for reliable RA design.

Figure 4 shows the radiation pattern of the 20 × 20 RA operating at f_0 = 10 GHz, designed using the inverse model. It should be emphasized that having the inverse model, the computational cost of RA design is negligible.

B. EXAMPLE 2: CENTER-HOLE UNIT CELL

Consider the unit cell shown in Fig. 5(a)-(b). The frequency of interest is again f_0 = 10 GHz. The parameter b = 15 mm is fixed, and the design space for the parameters $\boldsymbol{x}$ = [ε_r h g_1 g_2]^T, is $\boldsymbol{l}$ = [1.3 2.0 1.0 1.0]^T, and $\boldsymbol{u}$ = [2.7 20.0 7.0 7.0]^T. The cell volume is $V(\boldsymbol{x}) = b^2h - ((b-2g_1)^2 + (b-2g_1)(b-2g_2) + (b-2g_2)^2)h/3$.

The anchor designs corresponding to $P_{t.k}$ = –90°, …, –450°, were found by solving (1) at the total cost of 65 cell simulations. The minimum-volume designs are obtained for ε_r = 2.7, g_1 = g_2 = 1.0 mm in all cases. The optimum values of parameter h are $\boldsymbol{y}_2$ = [2.46 4.44 6.30 8.27 10.55 13.03 15.33] mm. The inverse model takes the form of $S_I(P)$ = [2.7 $I(P,\boldsymbol{P}_t,\boldsymbol{y}_2)$ 1.0 1.0]^T (cf. Fig. 5(c)). The average value of the absolute error of the model is only about 0.2°. Figure 6 shows the radiation pattern of the 20 × 20 RA operating at f_0 = 10 GHz, designed using the inverse model.

C. EXAMPLE 3: PYRAMIDAL-SHAPE UNIT CELL WITH CENTER HOLE

The final example is the unit cell shown in Fig. 7(a)-(b), also designed for f_0 = 10 GHz. We have $\boldsymbol{x}$ = [ε_r h a g c]^T, is $\boldsymbol{l}$ = [1.3 1.0 3.0 0.5 0.1]^T, and $\boldsymbol{u}$ = [2.7 20.0 15.0 1.0 0.9]^T, b = 15 mm is fixed. The cell volume is $V(\boldsymbol{x}) = (b^2 + ab + a^2)h/3 - hc(a-2g)^2$. The anchor designs corresponding to $P_{t.k}$ = –90°, …, –450°, were found by solving (1) at the total cost of 78 cell simulations.

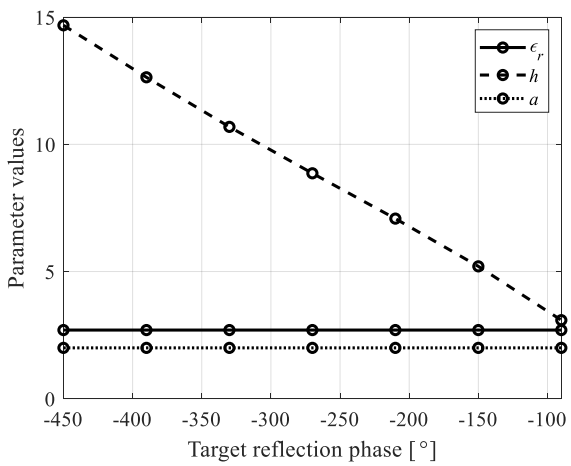

FIGURE 3. Plot of the inverse surrogate model for the unit cell of Fig. 2. Note that the model is constant for ε_r = 2.7, and a = 2.0 mm.

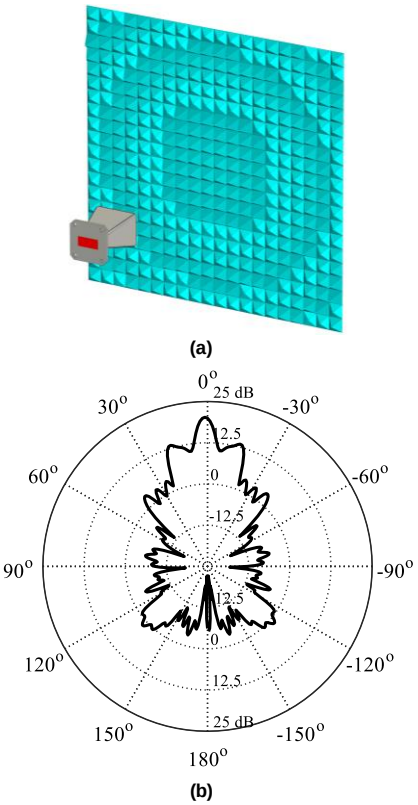

FIGURE 4. 20 × 20 RA designed using the inverse surrogate model developed for the unit cell of Fig. 2: (a) 3D view of the RA, (b) EM-simulated realized gain at f_0 = 10 GHz.

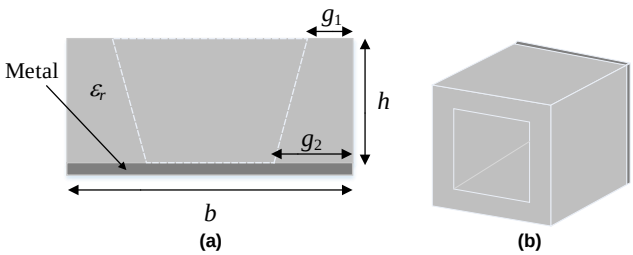

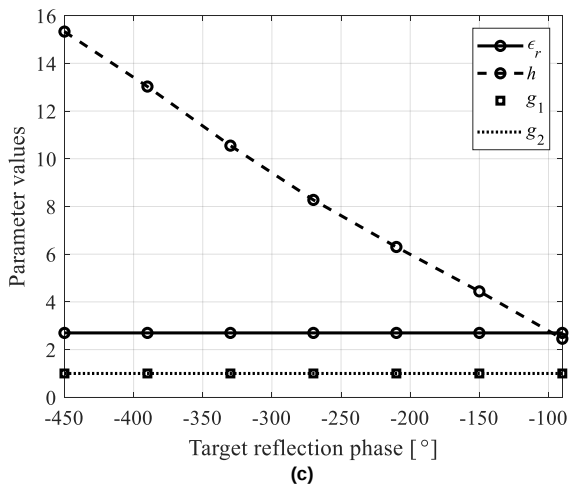

FIGURE 5. RA unit cell (Example 2): (a) parameterized side view, (b) perspective view. Note that the middle part of the cell is a hole parameterized by g_1 and g_2, and extending through the entire cell height; (c) inverse surrogate model; note that the model is constant for ε_r = 2.7, and g_1 = g_2 = 1.0 mm.

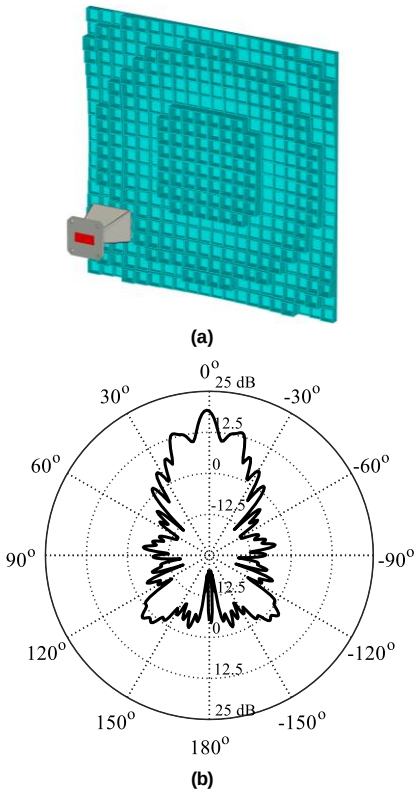

FIGURE 6. 20 × 20 RA designed using the inverse surrogate model developed for the unit cell of Fig. 5: (a) 3D view of the RA, (b) EM-simulated realized gain at f_0 = 10 GHz.

The minimum-volume designs are obtained for ε_r = 2.7, a = 3.0, g = 0.5, and c = 0.9 mm in all cases. The optimum values of parameter h are $\boldsymbol{y}_2$ = [1.24 3.09 4.74 6.42 8.21 10.21 12.31] mm. The inverse model takes the form of $S_I(P) = [2.7\ I(P,\boldsymbol{P}_t,\boldsymbol{y}_2)\ 3.0\ 0.5\ 0.9]^T$ (cf. Fig. 7(c)). The average value of the absolute error of the model lower than 0.2°. Figure 8 shows the radiation pattern of the 20 × 20 RA operating at f_0 = 10 GHz, designed using the inverse model.

V. EXPERIMENTAL VALIDATION

For further validation of the proposed design approach, one of the RA designs obtained in Section IV (Example 3) has been fabricated using a 3D printer and measured, cf. Fig. 9. The RA has been manufactured using RoboxDual by CEL – a dual material 3D printer [47] using Polylactic acid (PLA) 1.75mm 3D printing filament [48]. A 9 kHz-to-13.5 GHz Vector Network Analyzer, and LB-8180-NF broadband 0.8-to-18 GHz horn antenna, available at Yildiz Technical University have been used for the measurement. Figure 10 shows the simulated and measured radiation patterns, and cross-pol, co-pol characteristics of the RA prototype at 10 GHz. It can be observed that the experimental data (gain of 20.6 dBi) is well aligned with the simulations (21.7 dBi). The measured Side lobe level and aperture efficiency is obtained as -10.1 dB and 12% at 10 GHz. The performance of design can further improved by increasing the size array (increasing the total number of elements and size enlargement) and adjustment of the distance of the feed. Yet, it should be emphasized that the main goal of the work was to introduce a novel inverse surrogate modeling technique capable of providing low-cost models suitable for rapid EM-driven design optimization of reflectarray designs, rather than to proposing a novel reflectarray antenna design with high-performance characteristics.

Table 1 provides a computational performance comparison of the proposed approach and the FW-EM based-model. The simulations have been done using the following simulation setup: AMD Ryzen 7 3700X 8-Core Processor 3.59 GHz, with 32.0 GB of installed RAM, and NVidia 2080 GPU 8 GB. The descriptions of a single unit element model, and a complete array design model are given along with the total time required to obtain optimized array designs using both the FW-EM model and the proposed approach.

TABLE 1. Performance comparison of the proposed approach and FW-EM-model-based design in terms of the computational cost of individual simulations and total design process

Model	Model specifications	Simulation time
Single unit element in FW-EM simulator	Cells per wavelength & max model box edge= 20 Fraction of maximum cell near to model=25 Mesh size = 26,620	15 [Seconds]
Single run of inverse surrogate model	The surrogate model is generated using 78 cells using FW-EM model.	0.1 [Seconds]
Single run of FW-EM tool for the array in Section V with medium complexity mesh configuration	Cells per wavelength & max model box edge= 10 Fraction of maximum cell near to model=15 Mesh size = 3,437,100	8 [Minutes] [Calculated gain 22.3 dBi]
Single run of FW-EM tool for the array in Section V with high complexity mesh configuration	Cells per wavelength & max model box edge= 15 Fraction of maximum cell near to model=20 Mesh size = 8,892,720	15 [Minutes] [Calculated gain 21.7 dBi]
FW-EM based optimization of RA	Built-in Particle Swarm Optimization with swarm size of 45 and maximum iteration of 20, using uniform random distribution using medium complexity mesh configuration	120 [Hours] (8×901) [Obtained maximum gain 20.1 dBi]
Total design cost of the proposed approach	The optimally designed antenna is obtained via 400 (20 × 20) runs of inverse model and a single run of FW-EM tool for an array with high complexity mesh configuration	35.2 [minutes] (78×15 +400×0.1 + 15×60) [Obtained maximum gain 21.7 dBi]

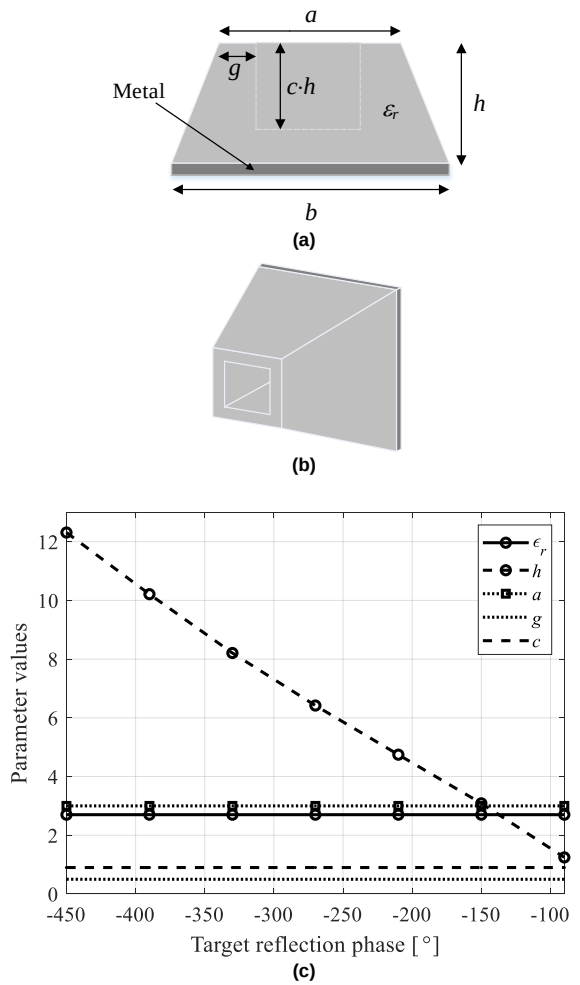

FIGURE 7. RA unit cell (Example 3): (a) parameterized side view, (b) perspective view. Note that the middle part of the cell is a hole parameterized by *g* and *c*, and extending into the cell height (depth of *c*·*h*); (c) inverse surrogate model; note that the model is constant for ε_r = 2.7, *a* = 3.0 mm, *g* = 0.5 mm, and *c* = 0.9.

The total cost of the proposed approach corresponds to 78 unit cell simulations necessary to obtain the anchor points for generating the surrogate model using the FW-EM simulation model (15 seconds), 400 evaluations of unit elements in the 20×20 array, and a single simulation of the entire array using high mesh configuration (for verification purposes). As it can be observed, the proposed method offers dramatic acceleration with respect to the FW-EM-based design approach. More specifically, it is almost 200 times faster (120 hours vs. 35.2 minutes). It should also be reiterated that from the method presentation perspective, the specific array designs considered here are merely illustration examples.

VI. CONCLUSION

This letter introduced a novel approach to EM-driven design of 3D-printed reflectarrays. It is based on inverse surrogate models constructed using pre-optimized anchor designs. The surrogate allows for a direct rendition of RA unit cell geometries featuring required reflection phases. Consequently, the cost of the entire design process corresponds to a few dozens of EM simulations of the unit elements (necessary for anchor design identification). This is at least an order of magnitude less than state-of-the-art surrogate-assisted methods.

Furthermore, a regularization-based formulation of the design task allows for ensuring uniqueness of solutions, as well as generation of minimum-volume geometries, which are desirable from the point of view of maintaining low weight and low fabrication cost of the RA. At the same time, regularization effectively reduces the design problem complexity by enforcing most of geometry parameters to be allocated the their lower or upper bounds. The design utility of our technique has been demonstrated both numerically and experimentally.

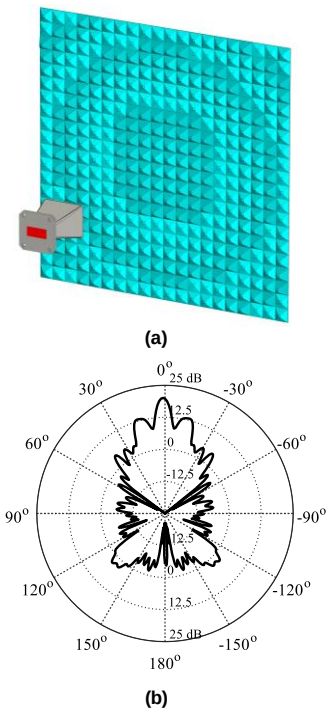

FIGURE 8. 20 × 20 RA designed using the inverse surrogate model developed for the unit cell of Fig. 8: (a) 3D view of the RA, (b) EM-simulated realized gain at f_0 = 10 GHz.

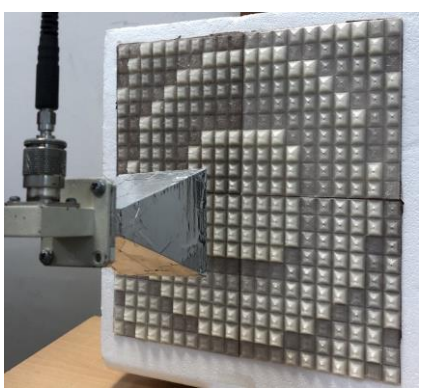

FIGURE 9. 20 × 20 RA designed using the inverse surrogate model developed for the unit cell of Fig. 8: a photograph of the 3D printed array prototype.

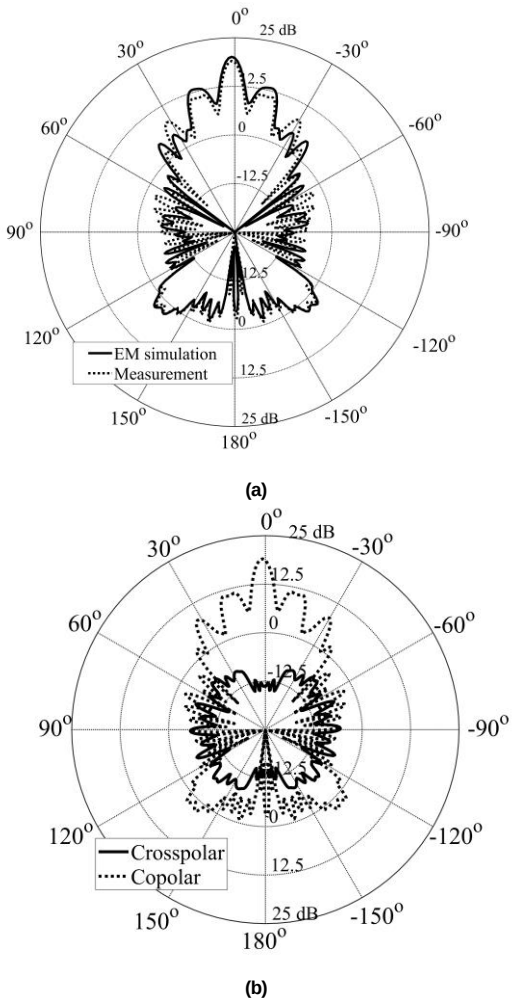

FIGURE 10. 20 × 20 RA designed using the inverse surrogate model developed for the unit cell of Fig. 9: (a) (b) EM-simulated and measured realized gain, (b) Measured Co-polar and Cross-polar radiation pattern, at f_0 = 10 GHz.

However, it should be emphasized that despite the mentioned advantages, similar to many methods reported in the literature, the proposed method also has its drawbacks. Since the proposed method is based on unit element characterization of reflectarrays elements, it is not possible to include effects such as mutual coupling in this approach. In other words, the discussed approach offers a trade-off between computational efficiency and reliability.

ACKNOWLEDGMENT

The authors would like to thank Dassault Systemes, France, for making CST Microwave Studio available. This work is partially supported by the Icelandic Centre for Research (RANNIS) Grant 206606 and by National Science Centre of Poland Grant 2020/37/B/ST7/01448.

REFERENCES

[1] F. Wu, R. Lu, J. Wang, Z. H. Jiang, W. Hong, and K. M. Luk, "A circularly polarized 1-bit electronically reconfigurable reflectarray based on electromagnetic element rotation," *IEEE Trans. Ant. Propag.*, vol. 69, no. 9, pp. 5585-5595, 2021.

[2] D. R. Prado, M. Arrebola, M. R. Pino, and G. Goussetis, "Broadband reflectarray with high polarization purity for 4K and 8K UHDTV DVB-S2," *IEEE Access*, vol. 8, pp. 100712-100720, 2020.

[3] C. A. Balanis, "Antenna Theory Analysis and Design," *4th Edition, John Wiley & Sons, Inc.*, New York, Chapter 14.10.

[4] A. Yu, F. Yang, A. Z. Elsherbeni, J. Huang, and Y. Kim, "An offset-fed X-band reflectarray antenna using a modified element rotation technique," *IEEE Trans. Ant. Propag.*, vol. 60, no. 3, pp. 1619–1624, 2012.

[5] G. Li, Y. Ge, and Z. Chen, "A compact multibeam folded transmitarray antenna at Ku-band," *IEEE Ant. Wirel. Propag. Lett*., vol. 20, no. 5, pp. 808-812, 2021.

[6] J. Wang, D. Li, S. Shang, D. Song, X. Luo, and X. Li, "Design of a folded reconfigurable reflectarray antenna for mono-pulse radar application," *12th International Symposium on Antennas, Propagation and EM Theory (ISAPE)*, Hangzhou, China, pp. 1-4, Feb. 2018.

[7] Z. Sun, Q. Chen, M. Guo, and Y. Fu, "Low-RCS reflectarray antenna based on frequency selective rasorber," *IEEE Ant. Wirel. Propag. Lett*., vol. 18, no. 4, pp. 693-697, 2019.

[8] J. A. Encinar, "Design of two-layer printed reflectarrays using patches of variable size," *IEEE Trans. Ant. Propag.*, vol. 49, no. 10, pp. 1403–1410, 2001.

[9] M. Chaharmir, J. Shaker, M. Cuhaci, and A. Ittipiboon, "Broadband reflectarray antenna with double cross loops," *El. Lett.*, vol. 42, no. 2, pp. 65–66, 2006.

[10] E. Carrasco, M. Barba, J. A. Encinar, M. Arrebola, F. Rossi, and A. Freni, "Design, manufacture and test of a low-cost shaped-beam reflectarray using a single layer of varying-sized printed dipoles," *IEEE Trans. Ant. Propag*., vol. 61, no. 6, pp. 3077-3085, 2013.

[11] M. Fazaelifar, S. Jam, and R. Basiri, "A circular polarized reflectarray antenna with electronically steerable beam and interchangeable polarizations," *Int. J. Microw. Wirel. Techn*., vol. 13, no. 2, pp. 198-210, 2021.

[12] J. Huang, and A. Feria, "A 1-m X-band inflatable reflectarray antenna," *Microw. Opt. Tech. Lett.*, vol. 20, no. 2, pp. 97-99, 1999.

[13] M. E. Bialkowski, A. W. Robinson, and H. J. Song, "Design, development, and testing of X-band amplifying reflectarrays," *IEEE Trans. Anten. Propag.*, vol. 50, no. 8, pp. 1065-1076, 2002.

[14] M. Moeini-Fard and M., Khalaj-Amirhosseini, "Nonuniform reflect-array antennas", *Int J RF and Microwave Comp Aid Eng*, vol. 22, no.5, pp. 575-580, 2012.

[15] Shi, Liping, Qinghe Zhang, Shihui Zhang, Guangxu Liu, and Chao Yi. "Accurate characterization of graphene reconfigurable reflectarray antenna element by SVR,"" IEEE Journal on Multiscale and Multiphysics Computational Techniques 6 (2021): 50-55.

[16] D. R. Prado et al., "Efficient crosspolar optimization of shaped- beam dual-polarized reflectarrays using full-wave analysis for the antenna element characterization," *IEEE Trans. Antennas Propag*, vol. 65, no. 2, pp. 623–635, Feb. 2017.

[17] R. T. Lee and G. S. Smith, "An alternative approach for implementing periodic boundary conditions in the FDTDmethod usingmultiple unit cells," *IEEE Trans. Antennas Propag.*, vol. 54, no. 2, pp. 698–705, Feb. 2006.

[18] R. Chiniard, A. Barka, and O. Pascal, "Hybrid FEM/floquet modes/PO technique for multi-incidence RCS prediction of array antennas," *IEEE Trans. Antennas Propag.*, vol. 56, no. 6, pp. 1679–1686, Jun, 2008.

[19] M. Salucci, L. Tenuti, G. Oliveri, and A. Massa, "Efficient prediction of the EM response of reflectarray antenna elements by an advanced statistical learning method," *IEEE Trans. Anten. Prop*., vol. 66, no. 8, pp. 3995-4007, Aug. 2018.

[20] Y. Mao, S. Xu, F. Yang, and A. Z. Elsherbeni, "A novel phase synthesis approach for wideband reflectarray design," *IEEE Trans. Antennas Propag.*, vol. 63, no. 9, pp. 4189–4193, Sep. 2015.

[21] R. Deng, F. Yang, S. Xu, and M. Li, "A low-cost metal-only Reflectarray using modified slot-type Phoenix element with 3600 phase coverage," *IEEE Trans. Antennas Propag.*, vol. 64, no. 4, pp. 1556–1560, Apr. 2016.

[22] L. Moustafa, R. Gillard, F. Peris, R. Loison, H. Legay, and E. Girard, "The Phoenix cell: A new reflectarray cell with large bandwidth and

rebirth capabilities," *IEEE Ant. Wirel. Propag. Lett.*, vol. 10, pp. 71–74, Jan. 2011.
[23] A. Vosoogh, K. Keyghobad, A. Khaleghi, and S. Mansouri, "A high efficiency Ku-band reflectarray antenna using single-layer multiresonance elements," *IEEE Ant. Wirel. Propag. Lett.*, vol. 13, pp. 891–894, Apr. 2014.
[24] R. Deng, S. Xu, F. Yang, and M. Li, "A single-layer high-efficiency wideband reflectarray using hybrid design approach," *IEEE Ant. Wirel. Propag. Lett.*, vol. 16, pp. 884–887, 2017.
[25] R. Deng, S. Xu, F. Yang, and M. Li, "Single-layer dual-band reflectarray antennas with wide frequency ratios and high aperture efficiencies using phoenix elements," *IEEE Trans. Ant Propag.*, vol. 65, no. 2, pp. 612–622, Feb. 2017.
[26] D. M. Pozar, S. D. Targonski, and H. D. Syrigos, "Design of millimeter wave microstrip reflectarrays," *IEEE Trans. Ant Propag.*,vol. 45, no. 2, pp. 287–296, Feb. 1997.
[27] P. Rocca, L. Poli, N. Anselmi, M. Salucci, and A. Massa, "Predicting antenna pattern degradations in microstrip reflectarrays through interval arithmetic," *IET Mirow. Ant. Propag.*, vol.10, no.8, pp. 817-826, June 2016.
[28] R. Deng, F. Yang, S. Xu, and M. Li, "An FSS-backed 20/30-GHz dual band circularly polarized reflectarray with suppressed mutual coupling and enhanced performance," *IEEE Trans. Ant Propag.*, vol. 65, no. 2, pp. 926–931, Feb. 2017.
[29] P. Nayeri, A. Z. Elsherbeni, and F. Yang, "Radiation analysis approaches for reflectarray antennas," IEEE Antennas Propag. Mag., vol. 55, no. 1, pp. 127–134, Feb. 2013.
[30] L. Marnat, R. Loison, R. Gillard, D. Bresciani, and H. Legay, "Accurate synthesis of a dual linearly polarized reflectarray," *3rd Eur. Conf. Antennas Propag. (EuCAP)*, Berlin, Germany, pp. 2523–2526, June 2009.
[31] G. Oliveri, A. Gelmini, A. Polo, N. Anselmi, and A. Massa, "System-by-design multiscale synthesis of task-oriented reflectarrays," *IEEE Trans. Ant. Prop.*, vol. 68, no. 4, pp. 2867-2882, 2020.
[32] A. Belen, F. Güneş, M. A. Belen, and P. Mahouti, "3D printed wideband flat gain multilayer nonuniform reflectarray antenna for X-band applications," *Int J Numer Modeling*, 33:e2753, 2020.
[33] D. R. Prado, J. A. López-Fernández, M. Arrebola, and G. Goussetis, "Support vector regression to accelerate design and crosspolar optimization of shaped-beam reflectarray antennas for space applications," *IEEE Trans. Ant. Propag.*, vol. 67, no. 3, pp. 1659-1668, 2019.
[34] D. R. Prado, J. A. López-Fernández, and M. Arrebola, "Systematic study of the influence of the angle of incidence discretization in reflectarray analysis to improve support vector regression surrogate models," *Electronics*, vol. 9, no. 12, pp. 2105, 2020.
[35] D. R. Prado, J. A. López-Fernández, M. Arrebola, and G. Goussetis, "On the use of the angle of incidence in support vector regression surrogate models for practical reflectarray design," *IEEE Trans. Ant. Propag.*, vol. 69, no. 3, pp. 1787-1792, 2021.
[36] L. Shi, Q. Zhang, S. Zhang, G. Liu, and C. Yi, "Accurate characterization of graphene reconfigurable reflectarray antenna element by SVR," *IEEE J. Multiscale Multiphys. Comp. Tech.*, vol. 6, pp. 50-55, 2021.
[37] P. Mahouti, M.A. Belen, N. Calik, and S. Koziel, "Computationally efficient surrogate-assisted design of pyramidal-shaped 3D reflectarray antennas," *IEEE Trans. Ant. Propag.*, Early Access, 2022.
[38] J. Huang, "Microstrip reflectarray," *Antennas and Propagation Society Symposium*, London, Canada, vol.2, pp. 612-615, 24-28, 1991.
[39] Y. Mao, S. Xu, F. Yang, and A. Z. Elsherbeni, "A novel phase synthesis approach for wideband reflectarray design," *IEEE Trans. Ant. Propag.*, vol. 63, no. 9, pp. 4189–4193, 2015.
[40] P. Nayeri, A. Z. Elsherbeni, and F. Yang, "Radiation analysis approaches for reflectarray antennas," *IEEE Ant. Propag. Mag.*, vol. 55, no. 1, pp. 127–134, 2013.
[41] P. Rocca, L. Poli, N. Anselmi, M. Salucci, and A. Massa, "Predicting antenna pattern degradations in microstrip reflectarrays through interval arithmetic," *IET Mirow. Ant. Propag.*, vol.10, no.8, pp. 817-826, 2016.
[42] R. Deng, F. Yang, S. Xu, and M. Li, "An FSS-backed 20/30-GHz dual band circularly polarized reflectarray with suppressed mutual coupling and enhanced performance," *IEEE Trans. Ant. Propag.*, vol. 65, no. 2, pp. 926–931, 2017.
[43] U. Ullah, S. Koziel, and I.B. Mabrouk, "Rapid re-design and bandwidth/size trade-offs for compact wideband circular polarization antennas using inverse surrogates and fast EM-based parameter tuning," *IEEE Trans. Ant. Prop.*, vol. 68, no. 1, pp. 81-89, 2019.
[44] A. Pietrenko-Dabrowska and S. Koziel, „Computationally-efficient design optimization of antennas by accelerated gradient search with sensitivity and design change monitoring," *IET Microwaves Ant. Prop.*, vol. 14, no. 2, pp. 165-170, 2020.
[45] S. Koziel and A. Pietrenko-Dabrowska, "Expedited optimization of antenna input characteristics with adaptive Broyden updates," *Eng. Comp.*, vol. 37, no. 3, 2019.
[46] S.P. Venkateshan and P. Swaminathan, *Computational Methods in Engineering*, Academic Press, Oxford, UK, 2013.
[47] S. Zhang, "Three-dimensional printed millimetre wave dielectric resonator reflectarray," *IET Microwaves Ant. Prop.*, 11(14), 2005-2009.
[48] J. Yang, Q. Cheng, M. K. T. Al-Nuaimi, A. Kishk and A. -E. Mahmoud, "Broadband Folded Reflectarray Fed by a Dielectric Resonator Antenna," *IEEE Ant. Wirel. Propag. Lett.*, vol. 19, no. 1, pp. 178-182, Jan. 2020.
[49] P. Nayeri, F. Yang, and A. Z. Elsherbeni, "Reflectarray Antennas: Theory, Designs, and Applications," *Hoboken, NJ, USA: Wiley*, 2018.
[50] P. Nayeri *et al*., "3D Printed Dielectric Reflectarrays: Low-Cost High-Gain Antennas at Sub-Millimeter Waves," *IEEE Trans. Ant. Prop.*, vol. 62, no. 4, pp. 2000-2008, April 2014.
[51] Y. -X. Sun, D. Wu and J. Ren, "Millimeter-Wave Dual-Polarized Dielectric Resonator Reflectarray Fabricated by 3D Printing With High Relative Permittivity Material," in *IEEE Access*, vol. 9, pp. 103795-103803, 2021.
[52] P. Nayeri and G. Brennecka, "Wideband 3D-Printed Dielectric Resonator Antennas," *2018 IEEE Int. Symp. Ant. Prop. & USNC/URSI Nat. Radio Sci. Meeting*, Boston, MA, USA, 2018, pp. 2081-2082.
[53] P. Nayeri and G. Brennecka, "Design of Flat Dielectric Reflectarrays Using State-of-the-Art Additive Manufacturing," *2018 IEEE Int. Symp. Ant. Prop. & USNC/URSI Nat. Radio Sci. Meeting*, Boston, MA, USA, 2018, pp. 1185-1186.
[54] RoboxDual by CEL – A Dual Material 3D printer, https://cel-uk.com/shop/roboxdual-by-cel-a-dual-material-3d-printer/, available on (16.08.2022).
[55] PLA 1.75mm 3D printing filament, https://cel-uk.com/shop/pla/, available on (16.08.2022).

SLAWOMIR KOZIEL received the M.Sc. and Ph.D. degrees in electronic engineering from Gdansk University of Technology, Poland, in 1995 and 2000, respectively. He also received the M.Sc. degrees in theoretical physics and in mathematics, in 2000 and 2002, respectively, as well as the PhD in mathematics in 2003, from the University of Gdansk, Poland. He is currently a Professor with the Department of Engineering, Reykjavik University, Iceland. His research interests include CAD and modeling of microwave and antenna structures, simulation-driven design, surrogate-based optimization, space mapping, circuit theory, analog signal processing, evolutionary computation and numerical analysis.

MEHMET ALI BELEN received his Ph.D degree in Electronics and Communication engineering from the Yıldız Technical University in 2016. He is currently an Associated Prof. in İskenderun Technical University. His current research interests are in the areas of multivariable network theory, device modeling, computer aided microwave circuit design, monolithic microwave integrated circuits, and antenna arrays, active/passive microwave components especially in the field of metamaterial-based antennas and microwave filters.

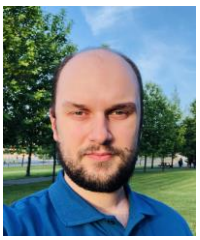

Alper Çalışkan received his Ph.D degree in Electronics and Communication Engineering from the Yıldız Technical University in 2019. He is currently a research assistant in Yıldız Technical University. The main research areas are optimization of microwave and millimeter wave antennas, ultra wideband antennas, radar systems, and computer aided circuit design.

PEYMAN MAHOUTI received his M. Sc. And Ph.D. degree in Electronics and Communication Engineering from the Yıldız Technical University, Turkey, in 2013 and 2016, Respectively. He is currently an Associated Professor with the Department of Aviation Electronics in Yıldız Technical University, Turkey. The main research areas are analytical and numerical modelling of microwave devices, optimization techniques for microwave stages, and application of artificial intelligence-based algorithms. His research interests include analytical and numerical modelling of microwave and antenna structures, surrogate-based optimization, and application of artificial intelligence algorithms.